

## 2D mobile breather scattering in a hexagonal crystal lattice

J. Bajars<sup>(1)</sup>, J. C. Eilbeck<sup>(2,3)</sup>, and B. Leimkuhler<sup>(2,4)</sup>

<sup>1</sup> Faculty of Physics, Mathematics and Optometry, University of Latvia,  
Jelgavas Street 3, Riga, LV-1004, Latvia

<sup>(2)</sup>Maxwell Institute,

<sup>(3)</sup>School of Mathematics, University of Edinburgh  
James Clerk Maxwell Building, The King's Buildings,  
Mayfield Road, Edinburgh EH9 3JZ, UK,

<sup>(4)</sup>Department of Mathematics, Heriot-Watt University,  
Riccarton, Edinburgh EH14 4AS, UK

(Dated: July 24, 2020)

### Abstract

We describe, for the first time, the full 2D scattering of long-lived breathers in a model hexagonal lattice of atoms. The chosen system, representing an idealized model of mica, combines a Lennard-Jones interatomic potential with an “egg-box” harmonic potential well surface. We investigate the dependence of breather properties on the ratio of the well depths associated to the interaction and on-site potentials. High values of this ratio lead to large spatial displacements in adjacent chains of atoms and thus enhance the two dimensional character of the quasi-one-dimensional breather solutions. This effect is further investigated during breather-breather collisions by following the constrained energy density function in time for a set of randomly excited mobile breather solutions. Certain collisions lead to 60° scattering, and collisions of mobile and stationary breathers can generate a rich variety of states.

The nature of mysterious particle-like tracks in muscovite mica crystals have attracted much recent interest [1]. The lines were first observed by Russell over 50 years ago [2], who suggested that they were caused by localized vibrational modes (which he called quodons) in the K-K layer of mica. This hypothesis has led to a number of simulations of breathers in model hexagonal lattices with on-site potentials [3–6]. The surprising conclusion of these studies is that in similar models in 2D, localized single breathers can travel along the main crystal directions of the lattice with little attenuation or lateral spreading.

In this note we move beyond the case of single breathers by examining breather-breather collisions. We present evidence that breathers are remarkably robust to collisions, and scattering through some multiple of 60° into another crystal direction is frequently observed in some circumstances. In addition we examine ensembles of initial conditions for breather-breather collisions to begin to understand how the relative angles and phases of the breathers affect their interactions.

Our simplified 2D model of the hexagonal K-K sheet layer in mica crystal [6] is based on the following dimensionless Hamiltonian which describes the classical dynamics of  $N$  potassium atoms:

$$H = K_E + U + V_c \quad (1)$$

$$= \sum_{n=1}^N \left( \frac{1}{2} |\dot{\mathbf{r}}_n|^2 + U(\mathbf{r}_n) + \frac{1}{2} \sum_{\substack{n'=1 \\ n' \neq n}}^N V_c(|\mathbf{r}_n - \mathbf{r}_{n'}|) \right),$$

where  $K_E$  is the kinetic energy,  $U$  is the on-site potential energy (modelling forces from atoms above and below the K-K sheet),  $V_c$  is the radial interparticle potential of the potassium atoms with a cut-off radius  $r_c$ ,  $\mathbf{r}_n \in \mathbb{R}^2$  is the 2D position vector of the  $n^{\text{th}}$  K atom,  $\dot{\mathbf{r}}_n$  is its time derivative, and  $|\cdot|$  is the Euclidean distance. Note that no motion in the  $z$ -direction is allowed. Any mention of “transverse” in the following means in-plane motion transverse to the breather propagation line.

The dimensionless on-site potential  $U$  is modelled as a smooth periodic function resembling an egg-box carton with hexagonal symmetry:

$$U(x, y) = \frac{2}{3} \left( 1 - \frac{1}{3} \left( \cos \left( \frac{2\pi(\sqrt{3}x-y)}{\sqrt{3}} \right) + \cos \left( \frac{2\pi(\sqrt{3}x+y)}{\sqrt{3}} \right) + \cos \left( \frac{4\pi y}{\sqrt{3}} \right) \right) \right), \quad (2)$$

where  $x$  and  $y$  are configurational coordinates,  $\mathbf{r}_n = (x, y)$ . Importantly, in any of the three crystallographic lattice directions with direction cosine vectors  $(1, 0)^T$  and  $(1/2, \pm\sqrt{3}/2)^T$ , the on-site potential (2) is a cosine, so the model reduces to a special case of the Frenkel-Kontorova model. The 1D atomic chains in the  $(1, 0)^T$  lattice direction are denoted by  $y_m$ , where  $m \in \mathbb{Z}$ . The interatomic interactions of K atoms are modelled by a scaled Lennard-Jones potential  $V_{LJ}(r)$  with cut-off radius  $r_c$ , i.e.

$$V_c(r) = \epsilon \left( \left( \frac{1}{r} \right)^{12} - 2 \left( \frac{1}{r} \right)^6 \right) + \epsilon \sum_{j=0}^4 A_j \left( \frac{r}{r_c} \right)^{2j}, \quad (3)$$

if  $0 < r \leq r_c$ , and zero elsewhere. The cut-off dimensionless coefficients  $A_j \rightarrow 0$  when  $r_c \rightarrow \infty$  are determined from matching and continuity conditions on  $V_{LJ}$  at well depth  $r = 1$  and the cutoff  $r_c$ , respectively, see [6] for more details.

In this paper we consider  $r_c = 3$  in dimensionless units. In general, we did not observe qualitatively different results for  $r_c \geq \sqrt{3}$ . This can be attributed to the rapid decay of the Lennard-Jones potential (3) for  $r \rightarrow \infty$ .

The dimensionless parameter  $\epsilon$  controls the relative strength of the two potentials. If  $\epsilon = 0$  then the system decouples into nonlinear oscillators whereas, for  $\epsilon \rightarrow \infty$ , the system behaves as a Lennard-Jones fluid. Previous studies [3] suggest that propagating breather solutions are observed when the two potentials are of roughly equal relative strength. For the system (1), mobile breather solutions can be observed [6] for  $\epsilon \in [0.001, 1]$ .

We mention here that other studies of hexagonal lattices have mostly concentrated on Morse lattices *without* an on-site potential, see for example [7, 8] and references therein. Ref. [8] discusses general cases of the so-called ‘‘crowdions’’, a modern name given to pulses called kinks in the older literature. Ref. [7] discusses solitons collisions with 2D scattering but the scattered pulses are not long-lived. Breather collisions are discussed in [9], but no cases involving  $60^\circ$  are described.

To excite mobile discrete breathers, the simplest method is to consider atoms in their dynamical equilibrium state, i.e. at the bottom of each well of the on-site potential (2), and excite three co-linear neighbouring atomic momenta in any crystallographic lattice direction with the pattern

$$\mathbf{v}_0 = \gamma(-1, 2, -1)^T, \quad (4)$$

where the values of  $\gamma \in \mathbb{R}$  depend on the choice of  $\epsilon$ . In contrast to other initial excitations such as single kicks or more complex patterns, we find that this pattern produces clean initial conditions for the excitation of mobile discrete breather solutions, i.e. produced very few phonons. Similarly, by considering patterns involving four co-linear atomic momenta  $\mathbf{w}_0 = \gamma(-1, 2, -2, 1)^T$ , we are able to excite stationary breathers. In the present study we concentrate on breather-breather interactions and therefore avoid the complications that a higher phonon density would bring.

We integrate the Hamiltonian dynamics of the system with the second order time reversible symplectic Verlet method [10, 11]. In the following, all numerical examples are performed with time step  $\tau = 0.04$  and periodic boundary conditions for different values of  $\epsilon$  and  $\gamma$ . We can define an energy density function by assigning to each atom its kinetic energy and on-site potential values as well as half of the interaction potential values. To obtain positive values we redefine  $H := H + |\min\{H\}|$  such that  $H \geq 0$ . In all energy density plots we interpolate  $H$  over a square uniform mesh.

The initial excitation (4) leads [6] to highly localized mobile breather solutions propagating on a chain of atoms in a crystallographic lattice direction with large displacements in the  $x$  direction, almost zero displacements in the  $y$ -axis direction and with small displacements in both axis directions on the chains of atoms adjacent to the main chain of atoms. In addition, the observed mobile breathers are optical with internal frequencies above the phonon linear spectrum.

In considering breather collisions, there are three possibilities. The first is inline or head-to-head collisions with two breathers on the same chain but travelling in opposite directions. These were first looked at briefly in [4]. The second occurs when two breathers approach each other along the same lattice vectors but on adjacent parallel chains. The third occurs when two breathers approach along different lattice vectors, i.e. at an angle of a multiple of  $60^\circ$ .

We discuss in detail elsewhere how the choice of  $\epsilon$  and  $\gamma$  affects the breather properties. In general increasing  $\gamma$  generates a narrower and faster moving breather in the direction of travel, but has little effect on the width of the breather perpendicular to the direction of travel. Increasing  $\epsilon$ , which also increases the speed, in contrast to the  $\gamma$  variable, increases the maximal displacements perpendicular to the direction of travel. This transverse spreading is important when discussing breathers colliding on adjacent, parallel tracks. In the present paper for conciseness, we consider only the values  $\epsilon = 0.01, 0.05$ .

The observations of mobile breather spectra and properties presented in [6] are demonstrated here with  $\epsilon = 0.05$  and a head-to-head collision shown in Figure 1. Consider a periodic lattice of size  $N_x = 400$  and  $N_y = 32$  of atoms in their equilibrium state and launch two atomic excitations (4) in the middle of the lattice at each ends of chain  $y_m$ . We indicate left and right excitation parameter values by  $\gamma_l$  and  $\gamma_r$ , respectively of opposite signs, to set the breathers on a collision course. We set  $\gamma_l = 0.4$  and  $\gamma_r = -0.5$ , and integrate in time until  $T_{end} = 1200$ . At around  $t = 700$ , the breathers collide, pass through and exchange some energy, see Figure 1.

In Figure 1(a) we plot the energy density function in time of the atoms on the main chain  $y_m$  where the greatest energy of the breather solution is localized. Notice the slight change in the breather propagation speed after the collision. This is also confirmed by the frequency spectrum plot in Fig. 1(b). Note also the breather frequency focusing in time before and after the collision, as was observed in [6]. Figure 1(b) clearly shows that the breather solutions have exchanged their energies and dominant internal frequencies during the collision.

The result of Figure 1 can be thought of as demonstrating a strongly one-dimensional nature, despite the 2D nature of the lattice. Due to the chaotic nature of molecular dynamics, the numerical observations, particularly at long times, are sensitive to changes in the initial

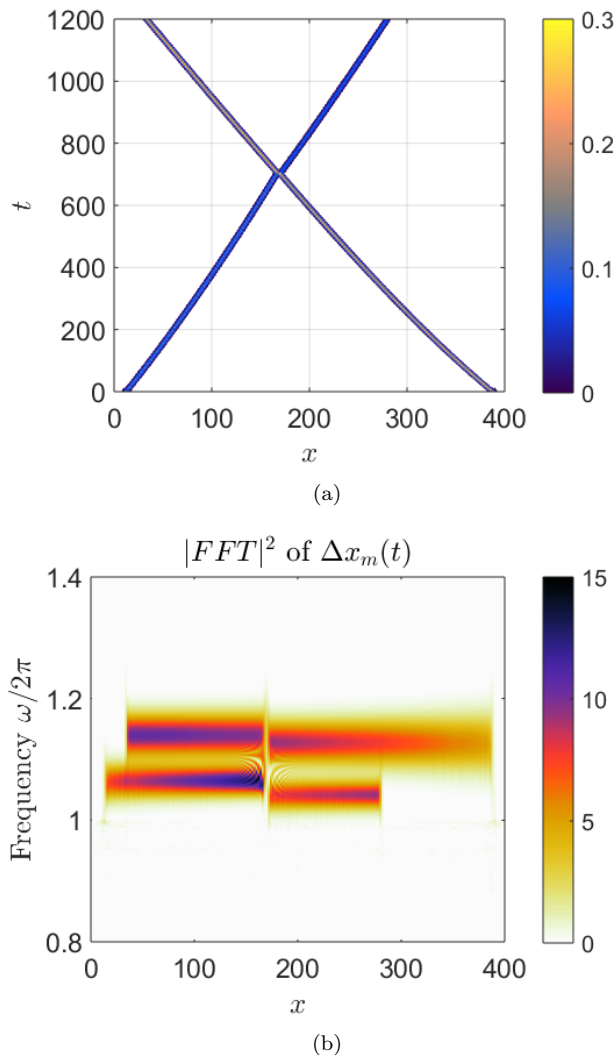


FIG. 1. Simulation of two mobile breather head-to-head collision. (a) energy density function on the main atomic chain of breather propagation. (b) frequency spectrum of atomic displacement function  $\Delta x_m(t)$  in  $x$ -axis direction from equilibrium.

conditions and to round-off error. This motivates us to consider an ensemble of initial conditions as well as different starting configurations, to study breather-breather collisions.

For the ensemble, we draw two sets of normally distributed random numbers  $X, Y \sim \mathcal{N}(0, 1)$  and scale them to normally distributed numbers with mean values  $\gamma_{l,r}$  and variance  $\sigma_{l,r}^2$ . Thus we obtain two sets of the excitation parameter value  $\gamma \sim \mathcal{N}(\gamma_{l,r}, \sigma_{l,r}^2)$  for numerical simulations. For the following examples on the lattice  $N_x = 200$  and  $N_y = 64$ , we consider two sets of 2000 random numbers sampling the standard Cauchy distribution (i.e. of the ratio  $X/Y$ ) and scale parameters equal to zero and one, respectively, with mean values  $\gamma_{l,r} = \pm 0.5$  and variances  $\sigma_{l,r}^2 = 0.002$ . Since a small amount of energy is

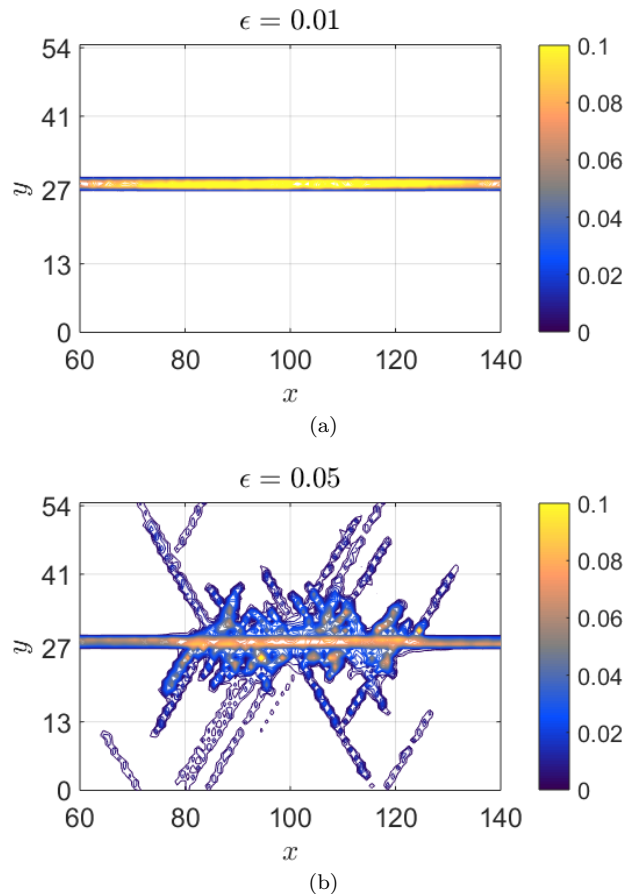


FIG. 2. Constrained ( $H > 0.01$ ) energy density function averaged over 50 time snapshots and 2000 individual simulations of breather-breather collisions on adjacent chains of atoms. (a) simulation with  $\epsilon = 0.01$  until  $T_{end} = 1000$ . (b) simulation with  $\epsilon = 0.05$  until  $T_{end} = 500$ .

present in the lattice, from phonons generated from the initial excitations, we set atomic energy density values to zero if the value is smaller than 0.01. This value is estimated from the numerical observations. Thus most of the phonon energy is disregarded for the final energy averages and most of the information comes from the breather solutions.

Using this set of initial velocities for *inline* collisions (as in Fig. 1) we did not observe scattering of breather solutions into different crystallographic lattice directions despite a visible spread of energy around the main chain of atoms of breather propagation. If instead we consider the scattering of two breathers on *adjacent* parallel lines, the results depend on the value of  $\epsilon$  used.

For  $\epsilon = 0.01$ , Fig. 2(a), we observed no scattering of breather solutions into different crystallographic lattice directions. However for  $\epsilon = 0.05$ , we observe breather scattering in all lattice directions, Fig. 2(b). Notice that dark energy lines arise *only* in these directions indicating propagating as well as stationary breather solutions. These examples demonstrate the 2D properties

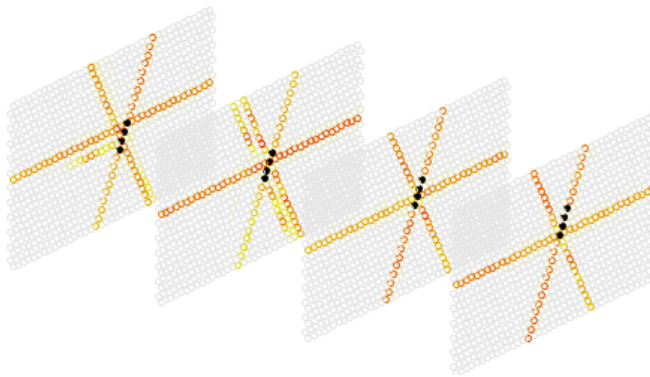


FIG. 3. Constrained ( $H > 0.01$ ) energy density function averaged over 50 time snapshots and 2000 individual simulations of mobile breather collisions with a stationary breather on a crystal axis at  $60^\circ$  to the moving one. The stationary breather is at slightly different positions in each case.

of breather solutions, breather energy scattering and the importance of the parameter  $\epsilon$ . Figure 2(b) confirms that the mobile breather's 2D character increases for larger values of  $\epsilon$ , that is, for a stronger interaction potential relative to a weaker on-site potential energy. Since Hamiltonian (1) is time reversible, Fig. 2(b) also demonstrates breather-breather collisions with an angle to each other when the time is reversed.

To explore further breather energy scattering by breather-breather collisions in 2D lattice model (1) we consider simulations of mobile breather collisions with a *stationary* breather at an angle to the incoming in Fig. 3. We consider four different locations of the  $(1, -2, 2, -1)$  stationary excitation pattern indicated by black circles.

For this experiment we consider a smaller size lattice,  $N_x = 120$  and  $N_y = 64$ , and integrate until  $T_{end} = 500$ . We consider a mean excitation value of  $\gamma_l = 0.5$  and  $\gamma_r = -0.35$  where  $\gamma_r$  refers to the stationary breather and variances  $\sigma_l^2 = 0.001$  and  $\sigma_r^2 = 0.00025$ . We used a much smaller variance value for the stationary breather compared to the moving one to ensure that the excitation is not too large to generate a mobile breather.

Because of the spread in incoming velocities/strengths etc., the relative *phases* of the two breathers will also be different in each simulation.

As above, we observe stronger breather energy scattering in the computations with  $\epsilon = 0.05$ , Fig. 3, in contrast to the simulations with  $\epsilon = 0.01$ , (not shown), where the scattering is predominately only in the lattice directions of both breathers.

Not only do we see scattering through a multiple of  $60^\circ$ , but the details of which track the breathers scatters to is

very sensitive to the velocity and phase of the incoming breather as well as the position of the stationary breather.

Our study has given us a better understanding of particle-like tracks in muscovite mica crystals. We demonstrate the importance of the relative strengths of the interatomic force and of the force from the surrounding atoms for the existence of long-lived propagating breathers and their 2D collision properties. Recent experimental work by Russell et al. [12] suggests strongly that breather-like objects are important in real 3D crystals of several different materials, displaying hyperconductivity and annealing effects at finite temperatures despite a range of defects such as impurities, dislocations, and crystal boundaries. We plan to extend the current model to one covering more realistic physical situations.

JB, during his postdoctoral research at the University of Edinburgh, and B JL acknowledge the support of the Engineering and Physical Sciences Research Council which has funded this work as part of the Numerical Algorithms and Intelligent Software Centre under Grant EP/G036136/1. JCE thanks Mike Russell for many useful conversations.

- 
- [1] J. F. R. Archilla *et al.*, eds., *Quodons in mica: nonlinear localized travelling excitations in crystals*, Springer Series in Materials Science, Vol. 221 (Springer International Publishing, 2015).
  - [2] F. M. Russell, *Nature* **216**, 907 (1967).
  - [3] J. L. Marín, J. C. Eilbeck, and F. M. Russell, *Physics Letters A* **248**, 225 (1998).
  - [4] J. L. Marín, J. C. Eilbeck, and F. M. Russell, in *Nonlinear Science at the Dawn of the 21st Century*, edited by P. L. Christiansen *et al.* (Springer, Berlin, 2000) pp. 293–306.
  - [5] J. Bajars, J. C. Eilbeck, and B. Leimkuhler, in [1] (2015) pp. 35–67.
  - [6] J. Bajars, J. C. Eilbeck, and B. Leimkuhler, *Physica D: Nonlinear Phenomena* **301**, 8 (2015).
  - [7] A. Chetverikov, W. Ebeling, and M. G. Velarde, *Letters on materials* **6**, 82 (2016).
  - [8] I. A. Shepelev, E. A. Korznikova, D. V. Bachurin, A. S. Semenov, A. P. Chetverikov, and S. V. Dmitriev, *Physics Letters A* **384**, 126032 (2020).
  - [9] A. A. Kistanov, V. D. Sergey, A. P. Chetverikov, and M. G. Velarde, *Eur. Phys. J. B* **87**, 211 (2014).
  - [10] M. P. Allen and D. J. Tildesley, *Computer Simulation of Liquids*, Oxford science publications (OUP, USA, 1989).
  - [11] B. Leimkuhler and S. Reich, *Simulating Hamiltonian Dynamics* (Cambridge University Press, 2005).
  - [12] F. M. Russell, M. W. Russell, and J. F. R. Archilla, *EPL* **127**, 16001 (2019).